

## VV PUPPIS: THE SOFT X-RAY MACHINE

JOSEPH PATTERSON, K. BEUERMANN,<sup>1</sup> D. Q. LAMB, G. FABBIANO, AND J. C. RAYMOND  
Harvard-Smithsonian Center for Astrophysics

AND

J. SWANK AND N. E. WHITE  
Goddard Space Flight Center

Received 1983 April 6; accepted 1983 September 9

## ABSTRACT

We report X-ray and ultraviolet observations of the AM Herculis-type binary VV Puppis, which show it to be a spectacular source at soft X-ray energies (0.1–0.3 keV), but only weakly detected in hard X-rays and in the ultraviolet. The orbital light curves in soft and hard X-rays are in good agreement with the mean optical light curve, indicating that essentially all the accretion luminosity originates from a small region ( $\lesssim 100$  km) near one of the magnetic poles of the white dwarf. An X-ray dip occurs once per binary period, when this region faces the Earth most directly; this is probably due to the absorption of soft X-rays in the accretion stream. The total energy distribution reveals four distinct components, peaking at infrared, optical/UV, soft X-ray, and hard X-ray energies. For a distance of 100 pc, the soft X-ray component has a luminosity  $L_{\text{sx}} = (3-20) \times 10^{31}$  ergs  $\text{s}^{-1}$  and a temperature  $kT = 23-43$  eV, while the hard X-ray component has a luminosity  $L_{\text{hx}} = (0.5-5) \times 10^{31}$  ergs  $\text{s}^{-1}$  and a temperature  $kT \gtrsim 5$  keV. The “optical plus UV” component has a luminosity  $\approx 6 \times 10^{31}$  ergs  $\text{s}^{-1}$ . For the most likely choice of parameters, the theoretical expectation  $L_{\text{sx}} \approx L_{\text{hx}} + L_{\text{cyc}}$  is approximately satisfied. Reconsideration of the observed fluxes in all four well-observed AM Her stars suggest that the “soft X-ray problem” may have disappeared. This can be more stringently tested by more accurate measurement of the temperatures of the soft and hard X-ray components.

*Subject headings:* stars: individual — X-rays: binaries

## I. INTRODUCTION

VV Puppis is one of 10 known AM Herculis close binary systems in which a magnetic white dwarf, rotating synchronously with the orbital period, accretes matter transferred from a low-mass companion (Chanmugam and Wagner 1977, 1978; Liebert *et al.* 1978). The surface magnetic fields of  $\sim 2 \times 10^7$  gauss are sufficient to channel the accretion flow onto the white dwarf's magnetic pole. Very high circular polarization is observed from the column of accreting material (Liebert *et al.* 1978), and is attributed to cyclotron radiation (Lamb and Masters 1979; Chanmugam and Dulk 1981; Meggitt and Wickramasinghe 1982). Efficient production of hard ( $\sim 20$  keV) and soft ( $\lesssim 0.1$  keV) X-rays is expected near the base of the column (Lamb and Masters 1979). Of the eight AM Her stars observed,<sup>2</sup> only VV Puppis has failed thus far to be detected as an X-ray source.

Detailed study of AM Her itself has led to a problem in understanding the overall energy distribution. Current models (Fabian, Pringle, and Rees 1976; Lamb and Masters 1979; Kylafis and Lamb 1979, 1982; King and Lasota 1979) attribute the soft X-rays to the heating of the white dwarf's magnetic polar cap by the intense flux of hard X-rays and/or cyclotron radiation emitted just above it. In this case, the luminosities of these three components should obey  $L_{\text{sx}} \approx L_{\text{hx}} + L_{\text{cyc}}$ . But

observations have suggested that the soft X-ray component is much more luminous than the hard X-ray or cyclotron sources (e.g., Tuohy *et al.* 1978, 1981; Raymond *et al.* 1979; Fabbiano *et al.* 1981). Intense soft X-ray fluxes are seen in essentially all other AM Her stars, suggesting that the phenomenon may afflict the entire class. This has created great difficulties for theory, and has become famous as “the soft X-ray problem.”

In this paper we report the detection of soft and hard X-rays from VV Pup, and present an orbital light curve for both. The light curves are in good agreement with the orbital light curve observed in the optical (Warner and Nather 1972, hereafter WN), suggesting that both X-rays and optical light arise from the vicinity of a bright spot near one magnetic pole of the white dwarf. The radius of the soft X-ray-emitting bright spot is in the range 20–120 km, and its temperature is in the range  $(2-6) \times 10^5$  K. The observed ratio of soft X-ray to hard X-ray fluxes is about 15, the highest of all the AM Her stars. Thus, it might seem to be the strongest example of the soft X-ray problem. But uncertainties in the temperatures of both components permit the ratio of luminosities  $L_{\text{sx}}/L_{\text{hx}}$  to range from 0.6 to 40, thus allowing  $L_{\text{sx}} \approx L_{\text{hx}}$ , in agreement with current models. In addition, the dominant source of optical light—known to be polarized, of very small extent, and located near the accreting pole—can also contribute to the production of soft X-rays by heating.

Reexamination of the X-ray data for the other three well-observed AM Her stars shows that in no case do the observations require extremely large soft X-ray luminosities.

<sup>1</sup> Also Max-Planck-Institut für Physik und Astrophysik, Institut für Extraterrestrische Physik, Garching bei München.

<sup>2</sup> Two of the newest members of the class, PG 1550+191 and CW 1103+25, have not yet been observed by any pointing X-ray telescope.

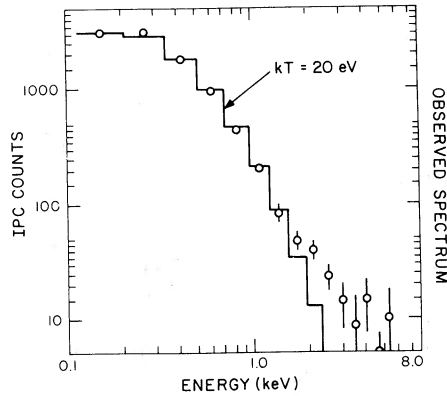


FIG. 1.—The IPC pulse-height spectrum of VV Pup. The soft component has been fitted by a 20 eV blackbody, but temperatures between 10 and 60 eV are admissible.

Thus, the soft X-ray problem may have vanished. However, if the blackbody temperature  $kT_{bb}$  is near the minimum allowed value in any of these systems, then the soft X-rays completely dominate the energetics, and  $L_{sx} \gg L_{hx} + L_{cyc}$ . The final disposition of the soft X-ray problem awaits more accurate measurement of  $kT_{bb}$  in each system.

## II. OBSERVATIONS

### a) X-Ray (IPC)

VV Puppis was observed for a total of 6000 seconds on 1980 April 20 with the imaging proportional counter (IPC) of the *Einstein Observatory* (see Giacconi *et al.* 1979 for a description of the telescope and detector). A very intense and very soft X-ray flux was detected. The preliminary calibration of the IPC pulse-height spectrum (Harnden 1980) yields the X-ray spectrum of Figure 1. The source is strong only below 1 keV, where the IPC energy resolution is too coarse to yield detailed spectral information. In Figure 1 we show the fit to a 20 eV blackbody for illustration. But with a liberal allowance for uncertainty in the IPC gain, we can set only limits of  $10 \text{ eV} \leq kT_{bb} \leq 60 \text{ eV}$  for the blackbody temperature of the soft component. We will narrow this range somewhat when we discuss the IPC spectral fitting in § III d. In addition, Figure 1 shows a weak hard X-ray flux (also detected by the MPC and SSS; see below) that cannot be produced by any reasonable tweaking of the model parameters which describe the soft X-ray flux. For an assumed 10 keV thermal bremsstrahlung spectrum, the observed 0.5–4.0 keV flux was  $\sim 3 \times 10^{-12} \text{ ergs cm}^{-2} \text{ s}^{-1}$ .

The individual light curves are shown at 10 s time resolution in Figure 2. They show rapid flickering with a time scale of  $\sim 200 \text{ s}$ , a slow hump extending from phase 0.75 to 0.2, and a deep minimum lasting  $\sim 100 \text{ s}$  near phase 0.95. Following standard practice in the literature on VV Pup, we have adopted Walker's (1965) orbital phase convention, *viz.*,

$$\text{Maximum light} = \text{JD}_{\odot} 2,427,889.6474 + 0.0697468256E. \quad (1)$$

The mean X-ray light curve, shown in Figure 3, was obtained by folding the three light curves on the orbital period. Note that this light curve shows significant X-ray flux in the deep minimum near phase zero, whereas the individual light curves in Figure 2 were consistent with zero flux in the minimum.

Close inspection of Figure 2 reveals the reason: the dip is not completely stable in orbital phase, but drifts by at least 0.01 cycles. Also shown in Figure 3 is the mean 1970–1971 optical light curve, obtained in unfiltered light with a blue-sensitive photomultiplier tube by WN. Apart from the X-ray dip, the gross features of the X-ray and optical light curves are quite similar. However, it should be noted that most of the post-1976 light curves lack the severe asymmetry seen in the WN data.

### b) Orbital Phasing

Since Walker's photometric ephemeris is now nearly 20 years old, it is time to check its current validity. We have measured time of hump beginning, hump end, and maximum light in all the *B* or *V* light curves published since 1950, and adopted the earlier timings of maximum light listed by Thackeray, Wesselink, and Oosterhoff (1950). All the times have been estimated by visual inspection of the light curves; this is simple enough for a fairly symmetrical hump shape, but a few of the light curves are so asymmetric that the estimates of maximum light have little meaning. The mean timings for three epochs (1964, 1971, and 1977–1980) are shown in Table 1; and the entire set of timings of maximum light is reduced to an *O*–*C* diagram in Figure 4, relative to Walker's ephemeris. In this figure we have condensed the pre-1950 photographic

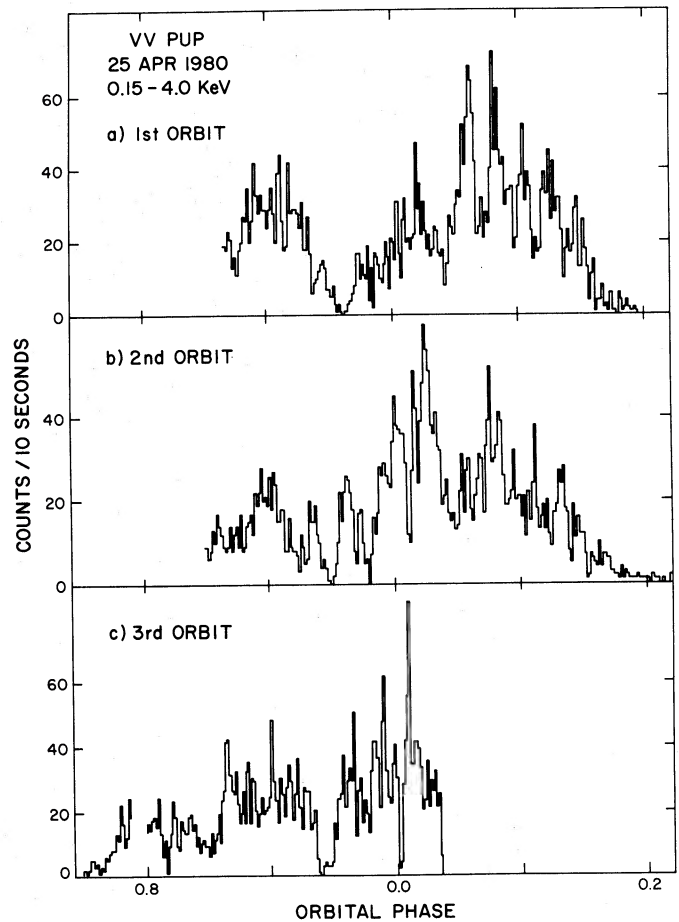


FIG. 2.—X-ray light curves of VV Pup at 10 s time resolution. Orbital phase has been calculated with eq. (1).

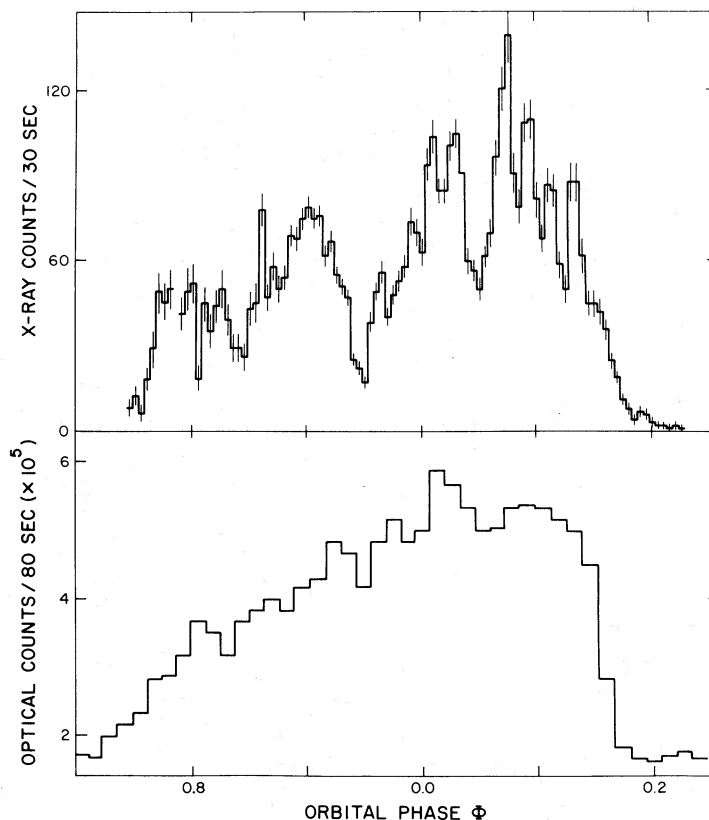


FIG. 3.—Mean X-ray and optical light curves. The optical light curve has been generated by measuring the five light curves published by WN, and averaging them. The error bars in the X-ray light curve refer to photon-counting errors only, not the variance of the individual measurements.

and visual timings into mean timings over a single year, or over several adjacent years. Where the mean is derived from five or more timings, the point is assigned high weight (*filled circle*); where the mean is derived from fewer timings, the point is assigned low weight (*open circle*). The post-1950 timings are all obtained from photoelectric light curves, and are therefore assigned high weight unless the light curves are severely asymmetric.

Figure 4 suggests that some small period or phase change may have occurred over the last decade, as previously noted by Liebert and Stockman (1979). This renders a proper accounting of the phase during the last decade uncertain by  $\sim 0.03$  cycles, and is especially bothersome since all of the important spectroscopic, polarimetric, and X-ray data were obtained during this interval. Until the nature of such phase changes is better understood, we will attempt to minimize confusion by adopting Walker's phase convention—noting

that the recent maxima have been occurring  $\sim 0.03$  cycles early.

### c) X-Rays (SSS)

VV Puppis was observed during the interval 1979 April 25–May 5 for a total of 19,000 seconds with the Solid State Spectrometer (SSS) of the *Einstein Observatory*. The source was too faint to extract useful spectral information, but the long observation enabled coverage of the entire orbital light curve, which is shown in two energy bands in Figure 5. Because the SSS is totally blind to very soft X-rays (such as the strong component seen in the IPC observation), these are the orbital light curves of the “hard component” of the X-ray source. Once again, they are very reminiscent of the optical light curve observed by WN. The mean flux in the 0.5–4.5 keV bandpass is  $8 \times 10^{-13}$  ergs  $\text{cm}^{-2}$   $\text{s}^{-1}$ , and a thermal bremsstrahlung fit yields  $kT \geq 3$  keV. There appears to be a very weak

TABLE 1  
PHOTOMETRIC EVENTS  
(Walker's ephemeris)

Source	Year	Start Hump	End Hump	Mid-Hump	Maximum Light
Walker .....	1964	0.787 (15)	0.187 (10)	0.987 (17)	0.013 (14)
WN .....	1971	0.763 (8)	0.188 (10)	0.975 (12)	0.040 (30)
Recent .....	1977–1980	0.740 (16)	0.188 (10)	0.963 (18)	0.975 (16)

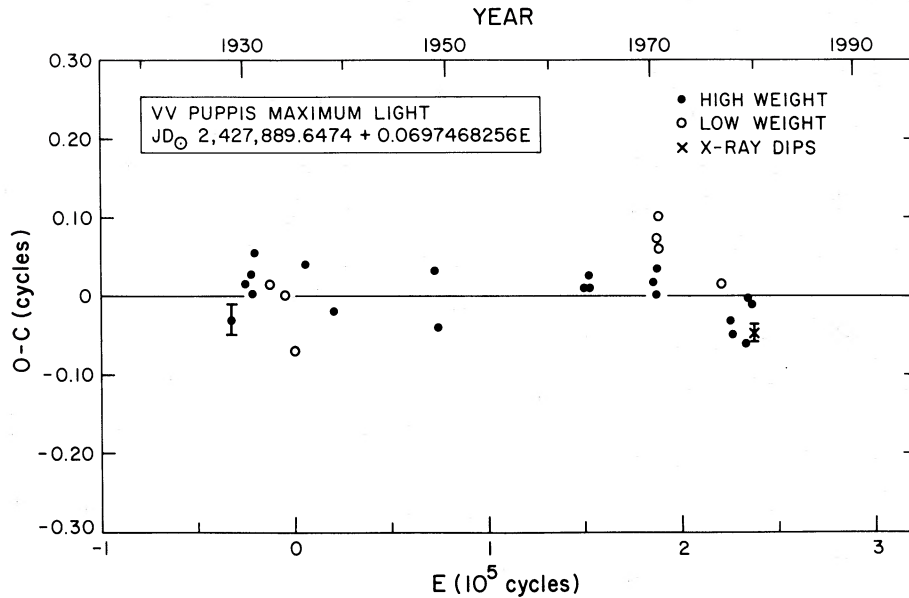


FIG. 4.—*O*—*C* diagram for optical timings of hump maximum, relative to Walker's ephemeris. Note that the recent timings appear to be systematically early.

detection during the “eclipse,” i.e., in the phase interval 0.2–0.75.

#### d) X-Ray (MPC)

For all of the X-ray observations, we have simultaneous coverage with the Monitor Proportional Counter (MPC), the hard X-ray “piggyback detector” on the *Einstein Observatory*. There were several detections of VV Pup at the  $3\sigma$  level; including nondetections, the average 2–6 keV flux was about  $2 \times 10^{-12}$  ergs  $\text{cm}^{-2} \text{s}^{-1}$ . A thermal bremsstrahlung fit yielded  $kT \geq 7$  keV, but the source was too weak to consider this limit trustworthy.

#### e) Ultraviolet

Short wavelength spectra of VV Pup in its bright state were obtained with the *International Ultraviolet Explorer* (see

Boggess *et al.* 1978 for details of the instrument) on 1980 June 30 and October 2. The first SWP 9407, is a 405 minute exposure (4 complete orbits of VV Pup), and is shown in Figure 6. Several bad data points were removed by using the line-by-line spectra; the 1980 May calibration (Bohlin *et al.* 1980) was used. The strongest emission lines are marginally overexposed in SWP 9407, but the errors introduced by saturation seem not to be large, since the line ratios agree quite well with those from the October spectrum, in which the lines are correctly exposed but the continuum very underexposed.

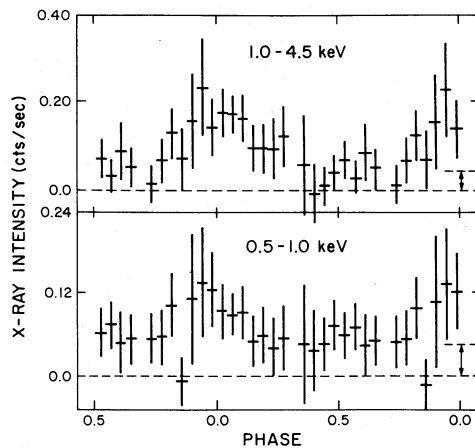


FIG. 5

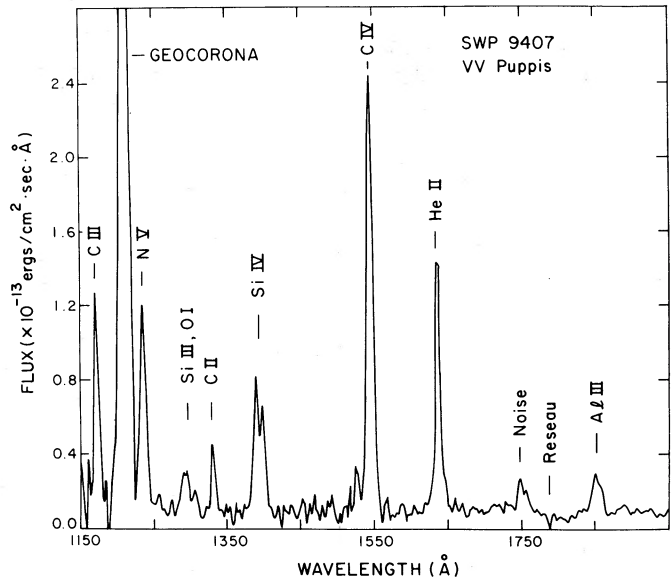


FIG. 6

FIG. 5.—SSS light curves folded at the orbital period. The long dashed line represents the estimated background level, and the short dashed line represents an extreme upper limit to the background level. An intensity of 0.20 counts  $\text{s}^{-1}$  corresponds approximately to a flux  $F(0.5\text{--}4.5 \text{ keV}) = 3 \times 10^{-12}$  ergs  $\text{cm}^{-2} \text{s}^{-1}$ .

FIG. 6.—The short-wavelength ultraviolet spectrum

TABLE 2  
ULTRAVIOLET FLUXES

ION	$\lambda$ (Å)	VV PUPPIS		AM HERCULIS
		SWP 9407	SWP 10267	
a) Line Fluxes ( $10^{-13}$ ergs $\text{cm}^{-2}$ $\text{s}^{-1}$ )				
C III	1176	9.9	...	30
N V	1240	10.4 <sup>a</sup>	3.9	52
Si III, O I	1300	2.2	...	9
C II	1335	2.0	...	13
Si IV	1400	8.8	3.2	54
C IV	1550	26.0 <sup>a</sup>	8.7	192
He II	1640	12.1	2.2	45
Al III	1860	2.8	...	20
Si III	1882	$\leq 0.6$	...	...
C III	1909	$\leq 0.3$	...	...
b) Continuum Fluxes ( $10^{-13}$ ergs $\text{cm}^{-2}$ $\text{s}^{-1}$ Å <sup>-1</sup> )				
	1270	0.13	b	3.0
	1360	0.10	b	2.3
	1435	0.09	b	2.1
	1487	0.11	b	2.0
	1590	0.09	b	1.8
	1670	0.11	b	1.7
	1710	0.11	b	1.7
	1780	0.11	b	1.6
	1900	0.10	b	1.4

<sup>a</sup> Marginally overexposed.

<sup>b</sup> Continuum fluxes about 3 times less than SWP 9407.

The latter spectrum, SWP 10267, is a 40 minute exposure during the faint phase ( $\phi = 0.3-0.7$ ), obtained on one side of the *IUE* large aperture. A second exposure during the bright phase was attempted immediately thereafter, but the error in the blind-offset position moved the star to the edge of the aperture, and no useful data were obtained. Thus, our first spectrum represents VV Pup averaged over an orbit, and the second represents the faint phase only.

Emission line and continuum fluxes in both spectra are presented in Table 2, with those of AM Her (Fabbiano *et al.* 1981) also listed for comparison. If VV Pup was in a similar state on the two dates, then the observed factor of 3 contrast in the continuum flux implies a factor of 5 contrast between the bright and faint phases of the orbital cycle.

### III. DISCUSSION

#### a) The Orbital Light Curve

Because the orbital period of VV Pup is very close to the 94 minute orbital period of the *Einstein Observatory*, the three IPC light curves only cover about half an orbital cycle. Nevertheless, Figures 2 and 3 make it clear that the X-rays track the mean optical light curve quite faithfully over the phase interval 0.75-0.2. A briefer IPC observation (not shown) on 1980 October 3 covered the phase interval 0.5-0.1, and also showed great similarity to the optical light curve, including the onset of the hump at  $\phi \sim 0.75$ . This is implicitly predicted by the model of Liebert *et al.* (1978), in which the optical light curve was attributed to the synchronous rotation of a small ( $\lesssim 100$  km) bright spot at one of the magnetic poles of the white dwarf. In fact, the soft X-ray light curves of all

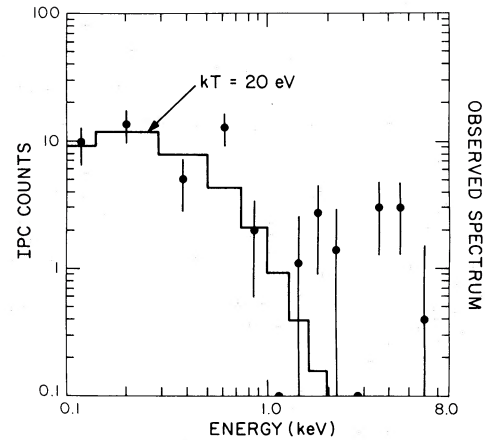


FIG. 7.—Mean IPC spectrum during the three X-ray dips. The spectrum appears harder, but a soft component is still strong.

well-observed AM Her stars (see discussion in § III f, below) are roughly consistent with such an origin, although two X-ray-emitting poles may be necessary for EF Eri and AN UMa. The apparent X-ray “eclipse” near phase 0.95 is very reminiscent of the periodic obscuration of the X-ray-emitting region by the accretion column seen in EF Eri (Patterson, Williams, and Hiltner 1981; White 1981). The eclipse in EF Eri also occurs near the middle of the X-ray-bright phase, drifts slightly in orbital phase, and shows a strong dependence on energy (it is total for energies below 0.8 keV, and absent above  $\sim 2$  keV). Is the X-ray dip in VV Pup similarly energy-dependent? We have attempted to answer this by fitting an X-ray spectrum to intervals within  $\pm 60$  s of the center of the dip. This yields a grand total of 53 photons, and in Figure 7 we show their X-ray spectrum. The spectrum is certainly harder than that of Figure 1, suggesting that absorption is in fact responsible for the dip. Our energy resolution at energies below  $\sim 0.5$  keV is so poor that we cannot specify the energy dependence of the absorption: the data can be fitted with normal photoelectric absorption by cool material, as well as with a uniform energy-independent veiling of the soft X-ray source. But in any case, the soft X-rays are strongly attenuated and the hard X-rays are not, so it seems reasonable to interpret this as an absorption effect. We shall henceforth refer to a “dip” rather than an eclipse, since the latter term has already been appropriated for the orbital phase interval 0.19-0.75.

#### b) Geometry of the System

The photometric observations at all wavelengths can be used to constrain the geometry of the system. From all of the published data we have obtained or estimated times for the various critical events around the orbit; these times and their corresponding phases are given in Table 3. Both X-ray and optical humps, and the X-ray dip, indicate that the accreting pole is most nearly face-on near  $\phi = 0.966 \pm 0.015$ . The infrared observations (Szkody and Capps 1980; Allen and Cheraschuk 1982; Szkody, Bailey, and Hough 1983) show that the secondary is at inferior conjunction at  $\phi = 0.09 \pm 0.02$ . Therefore, the geometry must be as pictured in Figure 8, in which the binary is fixed and the observer is thought to be rotating clockwise around the outside of the circle. In this

TABLE 3  
PHASING OF ORBITAL EVENTS  
(1977–1980 data only)

Event	Phase
Maximum light .....	0.974 (16)
Mid-hump .....	0.966 (18)
X-ray dips <sup>a</sup> .....	0.951 (10)
B component receding .....	0.983 (12)
S component receding .....	0.120 (12)
Infrared minimum .....	0.090 (25)
Linear polarization pulse .....	0.110 (10)
Begin positive circular polarization .....	0.750 (12)
End positive circular polarization .....	0.111 (8)
S component brightest .....	0.370 (40)

<sup>a</sup> Three dips at JD<sub>0</sub> 2,444,349.61666,  
2,444,349.68565, and  
2,444,349.75489.

geometry we obtain free explanations (no new hypothesis required) for several observed (Schneider and Young 1980, hereafter SY; Cowley, Crampton, and Hutchings 1982) spectroscopic features:

- (1) Why the broad emission lines (“B component”) are in maximum recession at  $\phi = 0.98$ : the gas near the base of the funnel is falling away from us.
- (2) Why the sharp emission lines (“S component”) are in maximum recession at  $\phi = 0.12$ : the gas near the top of the funnel, where the stream velocity is low, is falling away from us. The binary orbital motion of the gas will retard this phase by an amount  $\lesssim 90^\circ$ ; we interpret the close agreement in phase ( $0.12 \approx 0.09$ ) as indicating that the amplitude of streaming motion significantly exceeds the amplitude of orbital motion.

(3) Why the sharp emission lines are *strongest* at  $\phi = 0.37$ : that portion of the low-velocity stream which the X-ray source can illuminate is most favorably presented to us (the funnel itself is certainly opaque to soft X-rays, as demonstrated by the absorption dip).

Our geometry also explains, approximately, the phasing of the polarimetric features (Tapia 1977; Liebert and Stockman 1979):

(4) The onset of circular polarization at  $\phi = 0.75$ : at this moment, the accreting pole first appears around the limb of the white dwarf.

(5) The circular polarization falls through zero and the linear polarization pulse peaks at  $\phi = 0.11$ : at roughly this moment, the accreting pole disappears around the limb, as evidenced by the end of the optical and X-ray hump (at  $\phi = 0.19$ ). The delay of  $\sim 0.07$  cycles between the polarization pulse and the end of the hump is significant; however, Liebert *et al.* (1978) have offered a reasonable explanation for the discrepancy: if the luminous part of the accretion column has a finite height, the luminous part remains in view for a few minutes after the base of the column has disappeared around the white dwarf's limb.

These explanations seem a very substantial return for the hypothesis invested. The only real unexplained feature is the occasional severe asymmetry of the optical (and possibly the X-ray) hump. We can suggest no plausible explanation for it.

Were the sharp emission-line component to arise strictly from the red star (as suggested by SY), then the red star should be located 0.22 cycles earlier (at phase 0.87), leaving everything else in Figure 8 unchanged. The observed intensity and velocity variations of the S component are thoroughly consistent with this possibility. But we have rejected it because it leaves unexplained the double-humped infrared light curve, observed in the “low state” (Szkody, Bailey, and Hough 1983). Both the

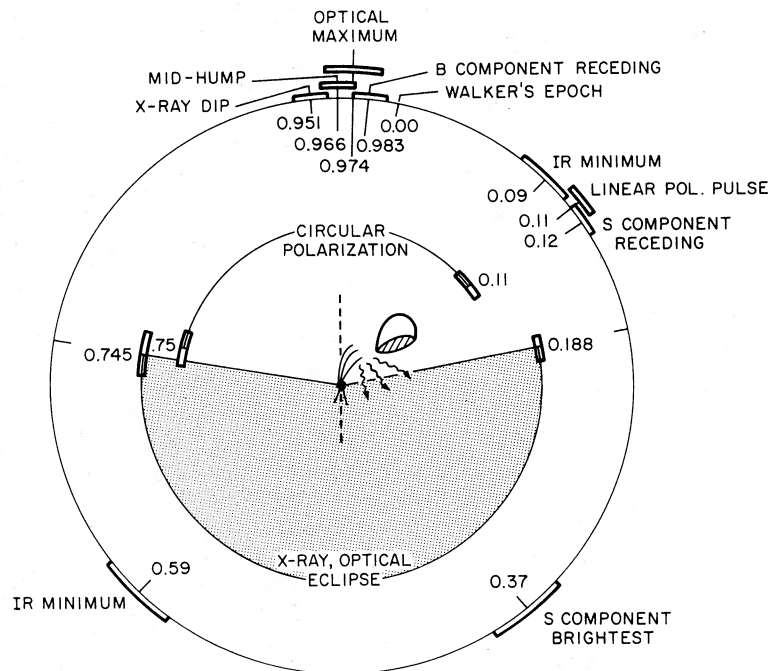


FIG. 8.—Phase diagram of events around the orbit, according to eq. (1). Here we keep the binary system fixed and imagine the observer to be moving clockwise around the circle.

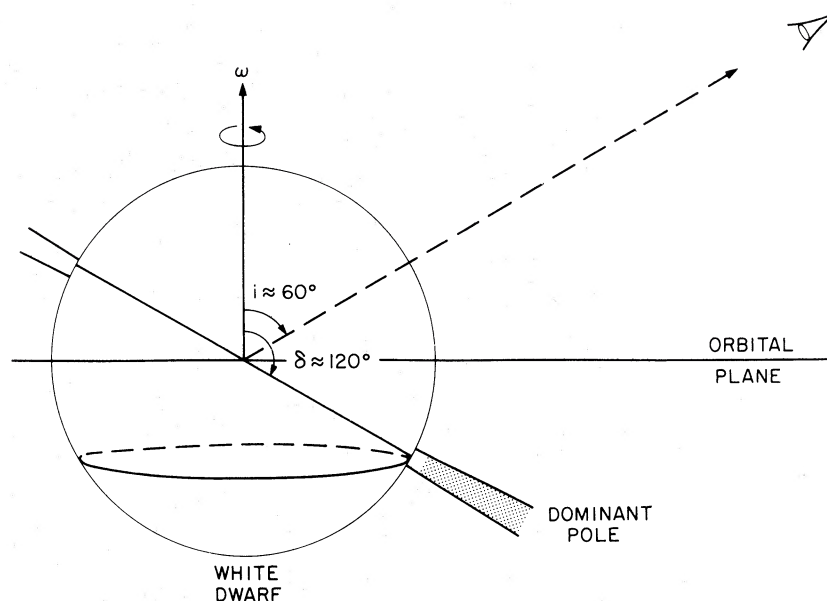


FIG. 9.—A close-up view of the white dwarf from the orbital plane at phase zero. The rotation axis and the observer are fixed in the plane of the paper. The magnetic axis describes the path shown by the dashed ellipse: at phase zero it is momentarily in the plane of the paper.

ellipsoidal wave form and the energy distribution in the low state provide evidence that this light comes from the secondary star. Since our adopted geometry explains the several facts listed earlier, including the observed intensity and velocity variations of the S component, and does not suffer from this objection, we favor it quite strongly.

Let us now estimate the orientation of the dominant accreting pole. In Figure 9, we show a close-up view of the white dwarf when the magnetic pole is most nearly facing the observer (phase  $\approx 0.00$ ). From the absence of true eclipse of the white dwarf by the secondary, we know that  $i$  must be less than  $\sim 75^\circ$ . To produce a hump lasting less than 0.5 cycles, the dominant accreting pole must lie on the hemisphere predominantly hidden from view, i.e., below the rotational equator. Hence, the colatitude  $\delta$  of the magnetic pole must satisfy  $\delta > 90^\circ$ , and more specifically a hump duration of 0.44 cycles implies  $\delta \approx 120^\circ$  for  $i \approx 60^\circ$ . These numbers agree roughly with more detailed modelling of the light curve and polarization behavior (Brainerd and Lamb 1984; see also Chanmugam and Dulk 1981), which give  $i = 75 \pm 5^\circ$ ,  $\delta = 150 \pm 5^\circ$ . (The difference between the two sets of angles arises from the fact that the latter analysis assumes that the dominant magnetic pole is visible for  $\Delta\phi = 0.37$ , derived from the circular polarization zero crossings, rather than  $\Delta\theta = 0.44$ , which we have used based on the duration of the optical and X-ray hump.)

Thus, we arrive at the surprising conclusion that when the magnetic axis points most nearly at the Earth (producing the X-ray and optical hump, and the X-ray dip), it is still  $50\text{--}70^\circ$  away from the line of sight! Where can the absorbing material responsible for the X-ray dip be? It seems very unlikely that it can be a portion of the accretion funnel near the magnetic pole, for three reasons: (1) absorption near the pole should produce a very broad dip, contrary to observation; (2) the intense hard and soft X-ray emission probably guarantees complete ionization of gas near the magnetic pole, preventing significant

absorption effects; and (3) if this portion of the funnel is anywhere near perpendicular to the star's surface, it just does not cross the line of sight.

Absorption in a portion of the funnel far from the X-ray emitting region is a much more promising possibility. In this case: (1) we expect a *narrow dip*, as observed; (2) we can understand how the absorption occurs, since the temperatures are relatively low (as evidenced by the optical H, He I, He II emission lines); and (3) there is a chance for some portion of the funnel to enter our line of sight to the X-ray-emitting region. We do not know the geometry of the accretion flow in detail, but it can easily be shown that the line of sight crosses the orbital plane at a height  $h$  above the white dwarf given by

$$h = R_* (\sin \delta - \cos \delta \tan i - 1),$$

where  $R_*$  is the white dwarf radius, and  $\delta$  and  $i$  are defined in Figure 9. For plausible values of  $\delta$  and  $i$ , we find that  $h$  is in the range  $0.5\text{--}4.0$  white dwarf radii. It remains for a more detailed analysis to consider whether some part of the stream could still be in the line of sight at this distance, but the possibility does not seem unreasonable to us. In any case, the existence of the absorption dip more or less *requires* that some portion of the accretion stream must extend quite far ( $\gtrsim 50^\circ$ ) from the magnetic axis of the white dwarf, as viewed from the magnetic pole.

### c) Ultraviolet Emission

The ultraviolet spectrum of Figure 6 shows more or less the normal set of emission lines seen in AM Herculis stars. Unlike the spectrum of AM Her, the continuum in Figure 6 is extremely flat, showing no signs of a very hot component ( $F_\lambda \propto \lambda^{-4}$ ) at short wavelengths. The flux of a Rayleigh-Jeans component at  $1300 \text{ \AA}$  must be less than  $2 \times 10^{-15} \text{ ergs cm}^{-2} \text{ s}^{-1} \text{ \AA}^{-1}$ ; this nondetection will be used below to constrain the temperature and emitting area of the region responsible for the soft X-ray emission.

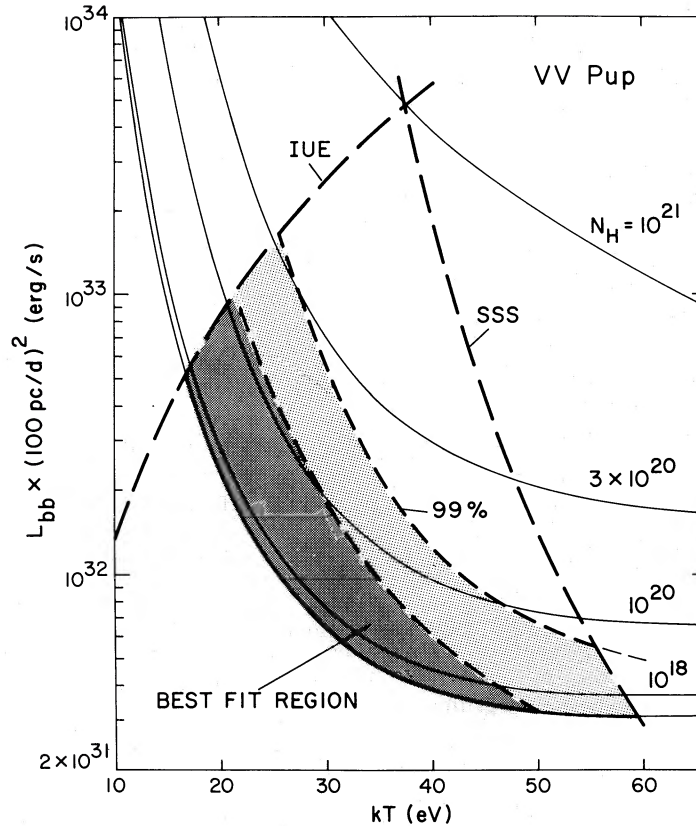


FIG. 10.—Constraints on the luminosity and temperature of the soft X-ray source, assumed to be a blackbody. Nondetections in the *IUE* and *SSS* constrain the source to be below the dash-dot lines. The allowed IPC spectral fits are in the shaded region, with the heavily shaded region preferred. Thin lines indicate the corresponding column density  $N_H$  in atoms  $\text{cm}^{-2}$ .

There is also a constraint on electron density available from the ratio of the C III lines  $I(1909)/I(1176)$ . It is very likely that the gas is photoionized by the intense soft X-ray emission, in which case the C III lines are formed at  $\sim 15,000$  K, and the excitation rates of Dufton *et al.* (1978) yield  $N_e \gtrsim 10^{14} \text{ cm}^{-3}$ . This is consistent with the lower limit of  $10^{12} \text{ cm}^{-3}$  obtained by Liebert *et al.* (1978).

#### d) The X-ray Spectrum

##### i) The Hard Component

All three detectors (IPC, SSS, MPC) reveal the existence of a source of hard X-rays, with an orbital light curve (see Fig. 5) apparently similar to the optical and soft X-ray orbital light curves. The mean 2–6 keV flux, averaged over the orbit, is  $\sim 1.5 \times 10^{-12} \text{ ergs cm}^{-2} \text{ s}^{-1}$ . For the temperature of the hard component, we have only the weak constraint  $kT > 5$  keV. Fitting the MPC hard X-ray flux with a thin bremsstrahlung spectrum yields a luminosity  $L_{br} \approx 2.2 \times 10^{31} (kT/30 \text{ keV})^{0.7} (D/100 \text{ pc})^2 \text{ ergs s}^{-1}$ .

##### ii) The Soft Component

The detection window of the IPC extends down to  $\sim 0.1$  keV, but the detector efficiency varies rapidly with energy near this limit. For sources with characteristic temperatures less than 40 eV, this problem (compounded by the very poor energy

resolution of proportional counters at such low energies) leads to an uncertainty in the observed flux of the soft component, and a much greater uncertainty in the total inferred luminosity of the soft component (assumed to have some characteristic spectrum, e.g., a blackbody). Of course, this lamentable problem is well known.

Formally, the IPC pulse-height spectrum of VV Pup can be acceptably fitted by blackbody temperatures in the range  $10 \text{ eV} < kT_{bb} < 60 \text{ eV}$ , within the uncertainties in IPC gain and the intervening column density  $N_H$  of absorbing material. Using the standard IPC spectral fitting programs, we have attempted to fit the pulse-height spectrum to model blackbody spectra with  $N_H$  and  $kT_{bb}$  to be determined. Since the value of the IPC gain is also free to vary within certain limits, it is quite cumbersome to show the resultant fits in a two-dimensional plot. But the important results are summarized in the temperature-luminosity diagram of Figure 10. For the entire permitted range of the IPC gain, the best-fit models are in the darkly shaded region. Models within the lightly shaded region are not a best fit for any permitted value of the gain, but are acceptable within 99% confidence limits. (The reason that no lightly shaded region exists at the bottom is that  $N_H = 0$  provides a firm lower bound to the solutions.) We have two additional constraints on a blackbody source: the nondetections in the SSS (say at 0.6 keV) and the *IUE* (say at

1300 Å).<sup>3</sup> Points above the dashed SSS and *IUE* curves in Figure 10 are thereby excluded.

It should be possible to constrain  $L_{\text{bb}}$  more tightly by using observations of reprocessed light from the secondary and/or accretion stream. The most useful constraint comes from the sharp component of the He II  $\lambda 4686$  emission, which is most readily produced by photoionization by soft X-rays. The recombination rate for He II  $\lambda 4686$  is  $\alpha_{4686} = 3.7 \times 10^{-13} \text{ cm}^3 \text{ s}^{-1}$ , compared with a total recombination rate  $\alpha_{\text{total}} = 1.44 \times 10^{-12} \text{ cm}^3 \text{ s}^{-1}$  (Osterbrock 1974). Thus 0.26 of all recombinations produce a  $\lambda 4686$  photon. Let us assume that the temperature of the EUV component is sufficiently high to produce most of its flux above the threshold to ionize He, viz., 54 eV. In particular, let us assume  $h\nu = 100 \text{ eV}$ . Then the luminosity of the He II sharp component should be approximately given by

$$L_{4686} = 0.26L_{\text{bb}}\Omega\left(\frac{2.65 \text{ eV}}{100 \text{ eV}}\right), \quad (2)$$

where  $L_{\text{bb}}$  is the luminosity of the blackbody component and  $\Omega$  is the fraction of the blackbody luminosity that falls on the emitting region. If the emitting region is the red star, then  $\Omega$  should be in the range 0.04–0.12, depending primarily on the unknown mass ratio. Since the emitting region is more likely to be the *stream*, a proper estimate of  $\Omega$  requires knowledge of how matter manages to leave the secondary (i.e., over what fraction of the star's surface).

At present no theory exists to specify this number, but there are observational reasons to believe that the stream probably subtends a solid angle at least equal to that subtended by the star itself. These reasons are:

1. *The X-ray absorption dip.* We have not offered a specific geometry to account for this event, but feel that it must signify the presence of absorbing material quite far from the line between the stars. In particular, since this material manages to occult the white dwarf while the red star *does not*, it probably subtends (at the white dwarf's magnetic pole) a solid angle greater than does the red star.

2. If the S component is produced by the stream and not the red star, then the question arises: Where is the expected contribution from the red star? In the geometry of Figure 8, we should see a very sharp component in maximum recession at  $\phi = 0.34$ . We estimate from the data of SY (their Fig. 5) that any such component must be  $\leq 20\%$  of the flux of the observed S component. There being no other plausible way to shield the red star, it seems probable that the stream itself intercepts most of the soft X-rays heading for the red star.

In the absence of further guidance from theory, we will simply assume that the stream subtends a solid angle equal to 1–2 times that subtended by the red star:  $\Omega = 0.06\text{--}0.18$ . From the data of SY, we estimate that the mean flux in the observed sharp component of He II  $\lambda 4686$  is  $\sim 8 \times 10^{-14} \text{ ergs cm}^{-2} \text{ s}^{-1}$ , during its period of visibility (orbital phase 0.15–0.6). Depending on how the reprocessing region is modelled, this implies that  $L_{4686}$  is in the range  $(4\text{--}10) \times 10^{28} (D/100 \text{ pc})^2 \text{ ergs s}^{-1}$ .

<sup>3</sup> We have assumed here, and will assume below, that all the "high state" observations can be directly compared. Since the brightness of VV Pup varies erratically with no truly stable state, this assumption introduces uncertainties of a factor of  $\sim 3$  when comparing observations made at different times.

From this constraint we obtain, using equation (2),

$$L_{\text{bb}} \approx (4\text{--}25) \times 10^{31} (D/100 \text{ pc})^2 \text{ ergs s}^{-1}. \quad (3)$$

From Figure 10 we then obtain a temperature

$$kT_{\text{bb}} = 30^{+14}_{-10} \text{ eV}. \quad (4)$$

We note that since the mean photon energy of a blackbody is  $2.8kT_{\text{bb}}$ , our assumption that most of the photons can ionize helium ( $> 54 \text{ eV}$ ) appears to have been justified.

Since we are attributing the soft X-ray emission to a slab of radius  $R$  on the white dwarf surface, we can write

$$L_{\text{bb}} = \pi R^2 \sigma T_{\text{bb}}^4, \quad (5)$$

from which we obtain

$$R = 62L_{32}^{1/2} T_{30}^{-2} \text{ km}, \quad (6)$$

$$f \approx 2 \times 10^{-5} L_{32} T_{30}^{-4},$$

$$L/f \approx 5 \times 10^{36} T_{30}^4 \text{ ergs s}^{-1},$$

where  $L_{32} = L_{\text{bb}}/10^{32} \text{ ergs s}^{-1}$ ,  $T_{30} = kT_{\text{bb}}/30 \text{ eV}$ , and  $f = \pi R^2/4\pi R_{\text{wd}}^2$ . We have taken  $R_{\text{wd}} = 7 \times 10^8 \text{ cm}$ , appropriate for a white dwarf of moderate mass. The most viable models yield a slab of radius 20–200 km, covering a fraction  $f \approx (0.5\text{--}50) \times 10^{-5}$  of the white dwarf's surface area. The corresponding  $L/f$  ratios are in the range  $(5\text{--}80) \times 10^{35} \text{ ergs s}^{-1}$ . For a white dwarf surface field of  $3 \times 10^7 \text{ gauss}$  (Visvanathan and Wickramasinghe 1979; Stockman, Liebert, and Bond 1979; Wickramasinghe and Visvanathan 1980), this places VV Pup in the regime where cyclotron losses and bremsstrahlung losses are expected to be approximately equal (see Fig. 4 of Lamb and Masters 1979).

#### e) Total Energy Distribution

In Figure 11, we present the complete energy distribution of VV Pup, averaged over the active phase of the light curve, i.e., the interval 0.75–1.19. For the hard X-rays, we show the emission for different choices of bremsstrahlung temperature. For the soft X-rays, we show the emission for three different choices of blackbody temperature  $kT_{\text{bb}}$ , corresponding to the three extreme corners of the allowed region in Figure 10. For the ultraviolet, we show the continuum data of Figure 6. For the optical and infrared, we show the data of Szkody, Bailey, and Hough (1983), Szkody and Capps (1980), and Allen and Cheraschuk (1982); and those of Liebert *et al.* (1978) for a low state observation.

In Figure 11 we identify four distinct components:

1. An infrared source which shows an apparently ellipsoidal light curve, an effective temperature of  $\sim 3000 \text{ K}$ , and fairly small variability (between high and low states, and around the orbit). In agreement with the above authors, we find it reasonable to identify this as predominantly the late-type star.

2. A polarized optical/UV source which dominates between 1000 and 9000 Å, and almost disappears during the low state; at least a large fraction of this can be identified plausibly as cyclotron radiation from the accretion funnel.

3. A blackbody soft X-ray source with  $kT_{\text{bb}} = 20\text{--}44 \text{ eV}$  and an emitting area  $\lesssim 10^5 \text{ km}^2$ , dominating between 10 and

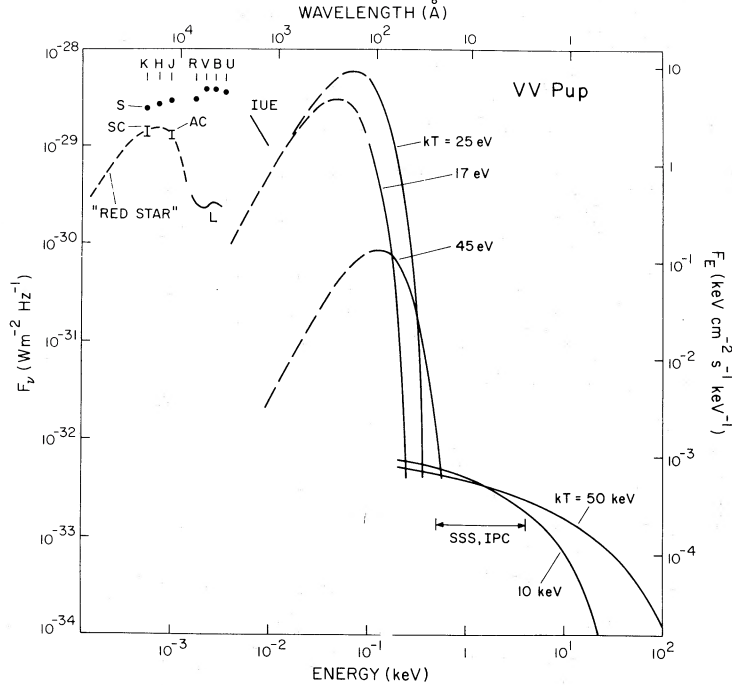


FIG. 11.—Composite energy distribution of VV Pup. The data for  $E > 5$  eV are presented in this paper (with three extreme models for the soft X-ray source corresponding to the three corners of the permitted region in Fig. 12). The filled circles indicate typical orbit-averaged values for the “bright state,” while the curved line labeled *L* represents the “low state.” The dashed line labelled *red star* is a cool blackbody fit to the infrared measurements in the low state.

400 eV; this could arise from the heating of the white dwarf surface by radiation emitted immediately above it.

4. A hard X-ray source with  $kT \geq 5$  keV, dominating beyond 0.5 keV, and producing an orbital light curve similar to the soft X-ray light curve; this probably arises from thermal bremsstrahlung in the accretion shock.

To convert the observed fluxes to luminosities, we require assumptions about the distance and the geometry of the emitting regions. It should be noted that the system geometry introduces two important uncertainties:

1. The radiation pattern of the soft X-ray emitting bright spot is different from that of the accretion column radiating hard X-rays and optical light.

2. The radiation pattern of the accretion column itself is not precisely known. In principle, hard X-rays should emerge from the column isotropically, but the published hard X-ray light curves of AM Her stars (especially those of AM Her and EF Eri) indicate that some angular dependence exists. It would be especially interesting to know what percent of the X-rays are emitted in the *downstream* direction (i.e., toward the magnetic pole), but of course we cannot ever observe the flux in this direction.

At present, these considerations are sufficiently serious that we can expect uncertainties of up to a factor of 4 or so to enter in converting observed fluxes to luminosities. Nevertheless, let us do the best we can. We will assume that the infrared emission is isotropic, and that the hard X-ray and optical/UV emissions are isotropic (but are intercepted by the body of the white dwarf for 56% of the orbital period). We will assume that the soft X-ray emission comes from a slab which is partially in view 44% of the period, and faces 60°

away from the line of sight at phase zero. Finally, we assume a distance of 100 pc. The component fluxes and resultant luminosities are shown in Table 4.

The hard X-ray temperature is a critical quantity, and poorly determined by our data. Only two AM Her stars have well-studied hard X-ray spectra: AM Her ( $kT = 31$  keV, Rothschild *et al.* 1981) and EF Eri ( $kT = 18$  keV, White 1981). Lacking good hard X-ray data, we will simply adopt  $kT = 30$  keV.

Current theories of accreting magnetic white dwarfs attribute the soft X-ray emission to a blackbody produced by the heating of the white dwarf's polar cap by hard X-ray and cyclotron radiation generated immediately above the pole. If the hard X-ray and cyclotron radiation is isotropic and the shock is very close to the surface, approximately half of the radiation strikes the surface, yielding  $L_{sx} \approx L_{hx} + L_{cyc}$ . It is evident that uncertainties in the modeling and in the value of  $kT_{bb}$  do

TABLE 4  
FLUXES AND LUMINOSITIES OF COMPONENTS IN VV PUPPIS

Source	Orbit-averaged Flux ( $10^{-11}$ ergs $cm^{-2}$ $s^{-1}$ )	$L$ (for $d = 100$ pc) ( $10^{31}$ ergs $s^{-1}$ )
Infrared.....	0.2	0.25
Optical/UV continuum.....	2.6	4.9
Optical/UV emission lines.....	1.0	1.2
Soft X-ray.....	1.5	3-100 <sup>a</sup> 4-25 <sup>b</sup>
Hard X-ray.....	0.12	$2.1(kT_{br}/30 \text{ keV})^{0.7}$

<sup>a</sup> From blackbody fit to X-ray spectrum only.

<sup>b</sup> From reprocessing argument of § III d.

not permit a sensitive test of this prediction. We can conclude only that  $L_{sx}/(L_{hx} + L_{cyc}) \approx 0.6-10$ , with a most probable value in the range 1-5. It does appear from Table 4 that the hard X-ray and optical/UV components should contribute about equally to the heating of the white dwarf's polar cap, if both originate from the postshock gas just above the pole.

### f) Comparison to Other AM Herculis Stars

#### i) AM Herculis Revisited

Analysis of the fluxes from AM Her has suggested that  $L_{sx} \gg L_{hx} + L_{cyc}$ . This has become famous as "the soft X-ray problem in AM Her," first pointed out by Tuohy *et al.* (1978), and later discussed by Raymond *et al.* (1979), Fabbiano *et al.* (1981), Fabbiano (1982), Rothschild *et al.* (1981), and Tuohy *et al.* (1981). The latter two discussions point out that the observational constraints on  $kT_{bb}$  and  $N_H$  for the soft X-ray source permit the  $L_{sx}/L_{hx}$  ratio to be as high as  $\sim 100$ , or as low as  $\sim 1$ . The possibility of very high values of  $L_{sx}/L_{hx}$  has attracted great interest, and has motivated the development of new theoretical models, in which much of the accretion energy is transmitted directly to the white dwarf, without the intermediary of hard X-ray or cyclotron radiation (Frank, King, and Lasota 1983; Kuipers and Pringle 1982).

The preliminary results of the *Einstein Observatory's* Objective Grating Spectrometer (OGS) observation favor somewhat higher temperatures and lower column densities ( $41 \text{ eV} < kT_{bb} < 55 \text{ eV}$ ,  $7 \times 10^{18} \text{ cm}^{-2} < N_H < 5 \times 10^{19} \text{ cm}^{-2}$ ; Heise and Brinkman 1982; Heise *et al.* 1984) than suggested by the earlier *HEAO 1* data. Actually, these values are close to the 90% confidence contours shown by Tuohy *et al.* (1981) for a 1978 pointed observation by *HEAO 1*, but disagree (primarily in  $N_H$ ) with the contours found in a 1977 scanning observation (Tuohy *et al.* 1978). It is not entirely clear how to interpret this discrepancy. But if we adopt the values of  $kT_{bb}$  and  $N_H$  found in the OGS observation, which is free from the difficult problems of spectral deconvolution, and a blackbody emission model, then about half of the total radiated soft X-ray/EUV flux appears in the 0.1-0.5 keV *HEAO 1* bandpass. Adopting the flux observed in the 1978 *HEAO 1* observation and an optically thick slab geometry (Rothschild *et al.* 1981), we find  $L_{sx} \approx (4-8) \times 10^{32} (D/100 \text{ pc})^2 \text{ ergs s}^{-1}$ . Assuming that the hard X-rays are emitted isotropically, the simultaneous 2-150 keV measurements yield  $L_{hx} = 4.9 \times 10^{32} (D/100 \text{ pc})^2 \text{ ergs s}^{-1}$ . If we adopt the flux from the 1975 *OSO 8* observation (Swank *et al.* 1977), we obtain slightly higher (but less well determined) luminosities, with  $L_{sx} \approx L_{hx}$  remaining true.

Thus, the soft X-ray problem in AM Her itself may have evaporated. There remains an ultraviolet problem, viz., the origin of the " $\nu^2$  component" which Raymond *et al.* (1979) located near the accretion bright spot. Since the observed flux in this component is relatively small ( $\sim 5 \times 10^{-11} \text{ ergs cm}^{-2} \text{ s}^{-1}$ ), this does not constitute a major problem in energetics unless its temperature is substantially above the lower limit of  $\sim 6 \text{ eV}$  available from the *IUE* data.

#### ii) The Overall Picture

The presence of soft X-ray absorption events in EF Eri and VV Pup provides a powerful constraint on geometrical models for these systems: the moment at which the line of sight to the accreting pole passes through the maximum column density is

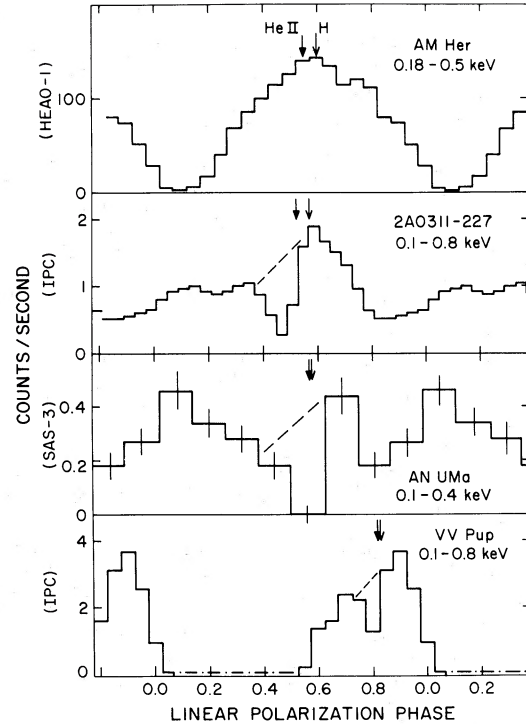


FIG. 12.—Soft X-ray light curves of AM Her stars in their "high states," with the data smoothed to reduce rapid variability. The dashed lines indicate intervals of assumed X-ray absorption. The dash-dot line for VV Pup indicates an interval not covered by the observations. The phases at which the broad components of the He II  $\lambda 4686$  and H $\beta$  emission lines reach maximum recessional velocity are indicated by the heavy and light arrows, respectively.

accurately specified. For purely radial accretion flow onto the pole (which must at least approximately hold, since the strong magnetic field must dominate the flow), this coincides with the moment at which the accretion funnel and the bright spot on the white dwarf surface point most directly at the Earth. In the simplest geometrical model of AM Her stars, two predictions follow directly: (1) in the absence of absorption effects, this should be the moment of soft X-ray maximum, since the spot presents maximum area at this time; and (2) the "broad component" of the emission lines, arising from infalling gas in the funnel, should reach maximum velocity of recession at this time.

These predictions are confronted with the observational data for the four well-observed AM Her stars in their "high states" in Figure 12. The orbital soft X-ray light curves are shown, with the dashed lines indicating intervals of X-ray absorption, and the arrows indicating the moment of maximum recessional velocity for the broad emission-line component. For each star but AN UMa, the time resolution in the original light curve has been degraded to reduce the effects of rapid flickering.<sup>4</sup> For each star, we have used an ephemeris for the linear polarization pulses, with the epoch given by Tapia (private communication) and the period given by the most recent spectroscopic work.

<sup>4</sup> As a consequence the light curves of EF Eri and VV Pup do not fall to zero intensity in the absorption dips, whereas the original light curves do.

TABLE 5  
OBSERVED ORBIT-AVERAGED CONTINUUM FLUXES OF  
AM HERCULIS STARS IN THE HIGH STATE

Bandpass	VV Pup <sup>a</sup>	AM Her <sup>a</sup>	2A0311-227 <sup>a</sup>	AN UMa <sup>a</sup>
$F_{sx}(0.1-0.5 \text{ keV})$ .....	15	400	40	28
$F_{hx}(2-6 \text{ keV})$ .....	1.2	40	25	<15
$F_{opt}(4000-7000 \text{ \AA})$ .....	3.3	45	6	6
$F_{uv}(1250-2000 \text{ \AA})$ .....	8	150	17	3
$F_{hx}(2-6 \text{ keV})$ .....	>3	300	150	...

<sup>a</sup> Units of  $10^{-12} \text{ ergs cm}^{-2} \text{ s}^{-1}$ .

As Figure 12 illustrates, all four stars show pronounced orbital variations (with AN UMa showing two maxima per orbit), and broad emission lines which reach maximum velocity of recession near the time of X-ray maximum. The two stars with demonstrable X-ray absorption dips show them at about the same time, and the dip in AN UMa at phase 0.55 may be a third example. Thus, the simple geometrical model, in which the X-ray humps, the X-ray absorption dips, and the redshifted emission lines all occur when we are gazing most directly at the accreting pole, passes this rather stringent test.

In Table 5 we present a simplified summary of the soft and hard X-ray fluxes of the four original members of the AM Her class. For simplicity we present only the orbit-averaged observed fluxes in four important and well-observed bandpasses, neglecting all considerations of geometry and model fitting. The primary sources are: VV Pup: this paper, Szkody, Bailey, and Hough (1983); AM Her: Rothschild *et al.* (1981), Fabbiano *et al.* (1981); 2A 0311-227: White (1981), Beuermann *et al.* (1984); AN UMa: Szkody *et al.* (1981), Hearn and Marshall (1979), Hartmann and Raymond (1980).

It is obvious that all four stars in the high state possess potent machines for producing soft X-ray luminosity; VV Pup and AM Her are the most extreme cases, with  $F_{sx}(0.1-0.5 \text{ keV})/F_{hx}(2-6 \text{ keV}) \approx 10$ . But, if the parameters of the soft X-ray emission seen by the OGS in AM Her are typical, then the observed soft X-ray flux represents most of the total, while the data for the best-studied stars, AM Her and 2A 0311-227, suggest that the total hard X-ray flux exceeds the 2-6 keV flux by a factor of  $\sim 7$ . These arguments imply that  $L_{sx}/L_{hx}$  is generally in the range 0.5-4. It is also noteworthy that the tabulated ultraviolet and optical fluxes (which must include the cyclotron component since the optical light is circularly polarized) are comparable to the observed soft X-ray flux, leaving open the possibility that heating by cyclotron radiation can contribute significantly to the soft X-ray luminosity. Thus, in all cases it appears entirely possible to power the soft X-ray source by reprocessing hard X-rays and/or cyclotron radiation on the white dwarf's surface. This hypothesis can be more severely tested by (1) more accurate determinations of  $T_{bb}$ , perhaps by objective-grating spectrometers on future X-ray telescopes; (2) simultaneous photometry in soft X-rays, hard X-rays, and optical light. Such studies should reveal a good correlation on short time scales, although it could be somewhat

masked by, for example, different angular dependences of these components.

#### IV. CONCLUSIONS

The IPC observation reveals that yet another AM Her star is an intense soft X-ray source. Among cataclysmic variables generally, strong soft X-ray emission is extremely rare; but every one of the observed AM Her stars is a strong source. This suggests that soft X-ray production may be as reliable a signature of the AM Her phenomenon as the optical polarization which defines it.

The soft and hard X-ray light curves in VV Pup agree with the predictions of the simplest model (Liebert *et al.* 1978), in which all of the accretion luminosity is released very near one magnetic pole of the white dwarf. We present a geometrical model which roughly accounts for the events occurring around the orbit, but at least three problems remain: (1) the occasional asymmetry of the X-ray/optical hump is unexplained; (2) the location of the red star is still not known with certainty (although we strongly favor the location shown in Fig. 8); and (3) we still do not know the reason for the X-ray absorption dip which occurs near phase zero.

The soft X-ray component in VV Pup is adequately fitted by a blackbody with a total luminosity  $L_{bb}$  in the range  $(3-100) \times 10^{31} (D/100 \text{ pc})^2 \text{ ergs s}^{-1}$ , and a temperature  $kT_{bb}$  in the range 17-50 eV. Reprocessing arguments, plausible but somewhat model-dependent, constrain these numbers more tightly:  $L_{bb} = (4-14) \times 10^{31} \text{ ergs s}^{-1}$ ,  $kT_{bb} = 23-43 \text{ eV}$ . The total luminosity at all other wavelengths is  $\sim 8 \times 10^{31} (D/100 \text{ pc})^2 \text{ ergs s}^{-1}$ , and therefore the soft X-ray component will dominate the energy budget if  $L_{bb}$  is near the upper end of its allowed range (corresponding to  $kT_{bb}$  near the lower end of its allowed range). This domination by soft X-rays has been thought to be true for AM Her, and is inconsistent with current theoretical models of radially accreting white dwarfs. But this conclusion is not warranted by current observations. From the overall energy budgets, AM Her now appears to be consistent with theory, and the other three stars might be, depending on the actual value of  $T_{bb}$ . Even VV Pup, which appears at first sight to contain the most potent soft X-ray machine of them all, turns out to be consistent with theory for the most likely choice of parameters ( $L_{bb} \approx 10^{32} \text{ ergs s}^{-1}$ ,  $kT_{bb} \approx 30 \text{ eV}$ ). It is tempting, though still somewhat premature, to conclude that the soft X-ray problem has disappeared, and that the simple models of white dwarf X-ray emission may have had it right in the first place.

We would like to thank John Heise, Steve Kahn, Jim Liebert, Keith Horne, Pete Stockman, and Santiago Tapia for helpful discussions. K. B. thanks the Smithsonian Astrophysical Observatory for hospitality and the Technical University of Berlin for leave of absence during the summer of 1982; he also thanks the Fulbright Commission for a travel grant. This research was supported in part by NASA grants NAGW-246 (DQL) and NAG 5-87 to the Smithsonian Institution.

#### REFERENCES

- Allen, D. A., and Cheraschuk, A. M. 1982, *M.N.R.A.S.*, **201**, 521.  
 Beuermann, K., *et al.* 1984, in preparation.  
 Boggess, A., *et al.* 1978, *Nature*, **275**, 372.  
 Bohlin, R. C., Holm, A. V., Savage, B. D., Snijders, M. A. J., and Sparks, W. M. 1980, *Astr. Ap.*, **85**, 1.  
 Brainerd, J. J., and Lamb, D. Q. 1984, in *Cataclysmic Variables and Low-Mass X-Ray Binaries*, ed. D. Q. Lamb and J. Patterson (Dordrecht: Reidel), in press.  
 Chanmugam, G., and Dulk, G. A. 1981, *Ap. J.*, **244**, 569.  
 Chanmugam, G., and Wagner, R. L. 1977, *Ap. J. (Letters)*, **213**, L13.

- Chanmugan, G., and Wagner, R. L. 1978, *Ap. J.*, **222**, 641.  
 Cowley, A. P., Crampton, D., and Hutchings, J. B. 1982, *Ap. J.*, **259**, 730.  
 Dufton, P. L., Barrington, K. A., Burke, P. G., and Kingston, A. E. 1978, *Astr. Ap.*, **62**, 111.  
 Fabbiano, G. 1982, *Ap. J.*, **262**, 709.  
 Fabbiano, G., Hartmann, L., Raymond, J., Steiner, J., Branduardi-Raymont, G., and Matilsky, T. 1981, *Ap. J.*, **243**, 911.  
 Fabian, A. C., Pringle, J. E., and Rees, M. J. 1976, *M.N.R.A.S.*, **173**, 43.  
 Frank, J., King, A. R., and Lasota, J. P. 1983, *M.N.R.A.S.*, **202**, 183.  
 Giacconi, R., et al. 1979, *Ap. J.*, **230**, 540.  
 Harnden, R. 1980, private communication.  
 Hartmann, L., and Raymond, J. C. 1980, in *The Universe at Ultraviolet Wavelengths*, ed. R. D. Chapman (NASA Conf. Pub. 2171), p. 495.  
 Hearn, D. R., and Marshall, F. J. 1979, *Ap. J. (Letters)*, **232**, L21.  
 Heise, J., and Brinkman, A. C. 1982, in *Galactic X-Ray Sources*, ed. P. W. Sanford, P. Laskarides, and J. Salton (Chichester: Wiley), p. 393.  
 Heise, J., Kruszewski, A., Chleboski, T., Mewe, R., Kahn, S., and Seward, F. D. 1984, in preparation.  
 King, A. R., and Lasota, J. P. 1979, *M.N.R.A.S.*, **188**, 653.  
 Kuipers, J., and Pringle, J. E. 1982, *Astr. Ap.*, **114**, L4.  
 Kylafis, N. D., and Lamb, D. Q. 1979, *Ap. J. (Letters)*, **228**, L105.  
 ———, 1982, *Ap. J. Suppl.*, **48**, 239.  
 Lamb, D. Q., and Masters, A. R. 1979, *Ap. J. (Letters)*, **234**, L117.  
 Liebert, J., and Stockman, H. S. 1979, *Ap. J.*, **229**, 652.  
 Liebert, J., Stockman, H. S., Angel, J. R. P., Woolf, N. J., Hege, E. K., and Margon, B. 1978, *Ap. J.*, **225**, 201.  
 Meggitt, S. M. A., and Wickramasinghe, D. T. 1982, *M.N.R.A.S.*, **198**, 71.  
 Osterbrock, D. E. 1974, *Astrophysics of Gaseous Nebulae* (San Francisco: Freeman), p. 67.  
 Patterson, J., Williams, G., and Hiltner, W. A. 1981, *Ap. J.*, **245**, 618.  
 Rappaport, S., Joss, P. C., and Webbink, R. F. 1982, *Ap. J.*, **254**, 616.  
 Raymond, J. C., Black, J. H., Davis, R. J., Dupree, A. K., Gursky, H., Hartmann, L., and Matilsky, T. A. 1979, *Ap. J. (Letters)*, **230**, L95.  
 Rothschild, R. E., et al. 1981, *Ap. J.*, **250**, 723.  
 Schneider, D. P., and Young, P. 1980, *Ap. J.*, **240**, 871 (SY).  
 Stockman, H. S., Liebert, J., and Bond, H. E. 1979, in *IAU Colloquium 53, White Dwarfs and Variable Degenerate Stars*, ed. H. M. Van Horn and V. Weidemann (Rochester: University of Rochester), p. 334.  
 Swank, J., Lampton, M., Bolt, E. M., Holt, S., and Serlemitsos, P. 1977, *Ap. J. (Letters)*, **216**, L71.  
 Szkody, P., Bailey, J. A., and Hough, J. H. 1983, *M.N.R.A.S.*, **203**, 749.  
 Szkody, P., and Capps, R. W. 1980, *A.J.*, **85**, 882.  
 Szkody, P., Schmidt, E., Crosa, L., and Schommer, R. 1981, *Ap. J.*, **246**, 233.  
 Tapia, S. 1977, *IAU Circ.*, No. 3054.  
 Thackeray, A. D., Wesselink, A. J., and Oosterhoff, P. Th. 1950, *Bull. Astr. Inst. Netherlands*, **11**, 193.  
 Tuohy, I. R., Lamb, F. K., Garmire, G. P., and Mason, K. O. 1978, *Ap. J. (Letters)*, **226**, L17.  
 Tuohy, I. R., Mason, K. O., Garmire, G. P., and Lamb, F. K. 1981, *Ap. J.*, **245**, 183.  
 Visvanathan, N., and Wickramasinghe, D. T. 1979, *Nature*, **281**, 47.  
 Walker, M. F. 1965, *Mitt. Sternw. (Budapest)*, No. 57.  
 Warner, B., and Nather, R. E. 1972, *M.N.R.A.S.*, **156**, 305 (WN).  
 White, N. E. 1981, *Ap. J. (Letters)*, **244**, L85.  
 Wickramasinghe, D. T., and Visvanathan, N. 1980, *M.N.R.A.S.*, **191**, 589.

K. BEUERMANN: Institut f. Astron. Astrophysik, Technische Universität, Berlin, Ernst-Reuter-Platz 7, D-1000 Berlin 10, West Germany

G. FABBIANO, D. Q. LAMB, JOSEPH PATTERSON, and J. C. RAYMOND: Center for Astrophysics, 60 Garden Street, Cambridge, MA 02138

J. SWANK: Code 661, Goddard Space Flight Center, Greenbelt, MD 20771

N. E. WHITE: European Space Agency-ESTEC, Postbus 299, NL-2200 Ag Noordwijken, The Netherlands